Nanoscale Horizons

ROYAL SOCIETY OF CHEMISTRY

COMMUNICATION

View Article Online
View Journal | View Issue

Cite this: *Nanoscale Horiz.*, 2025, **10**, 3416

Received 31st August 2025,
Accepted 22nd September 2025

DOI: 10.1039/d5nh00609k

rsc.li/nanoscale-horizons

Rational design of dynamic DNA self-assembly through a responsive-bond-embedded loop

Zhiyuan Zhu, Mengzhou Wei and Yulin Li *

Herein, we propose a versatile strategy for dynamic DNA self-assembly through a control loop embedded with responsive chemical groups. Responsive to a stimulus, the inserted chemical group will enable the formation or cleavage of the control loop, determining its intact or cleaved states. When the loop is intact, DNA self-assembly occurs; otherwise, the assembly process is prevented. The "Turn-On", "Turn-Off", and reversible "On–Off–On" systems have been achieved for two DNA assembly systems by incorporating different chemical groups, responding to various stimuli such as light irradiation, metal ions, and small molecules. The loop-controlled dynamic DNA self-assembly strategy holds excellent designability and versatility, enriching the existing regulation reservoir and bringing new opportunities for dynamic DNA nanotechnology.

New concepts

This work demonstrates the novel concept of taking advantage of the intact or cleaved states of a single-stranded loop to dynamically regulate DNA self-assembly. Responsive chemical groups are embedded in the control loop to regulate its states and hence realize the dynamic control of DNA self-assembly. In previous studies, responsive chemical groups were generally incorporated into the hybridization sequence. However, in our strategy, responsive chemical groups are embedded in the control loop which is not part of the hybridization sequence. Separating the control unit from the hybridization unit grants our strategy more designability and versatility. Besides, the control loop itself holds great potential for adding extra designability to the dynamic regulation systems of DNA self-assembly, in addition to the great variety of responsive chemical groups, opening up new possibilities for the development of dynamic DNA nanotechnology.

1. Introduction

Dynamic DNA nanotechnology has attracted worldwide interest since it holds great potential for a wide range of applications, such as *in vivo* sensing and therapy,[1–10] nanorobotics[11–19] and biocomputing.[20–24] One continuous pursuit is to develop various stimuli-responsive strategies to enrich the regulation pool, meeting the needs of diverse application scenarios.[25] One category of dynamic DNA systems takes advantage of the toehold-mediated strand displacement reactions or specific base sequences, such as aptamer, *i*-motif, G-quadruplex, *etc.*[26–34] Another important category achieves base-sequence-independent dynamic control by attaching stimuli-responsive chemical groups to the backbone of DNA strands.[35–41] The advantage of such strategies lies in the great diversity of chemical groups that can be used. Various stimuli, such as light irradiation, enzymes, small molecules and metal ions, have been employed for the dynamic control of DNA self-assembly by adopting different chemical groups. In the previous studies, the chemical groups were usually integrated in the hybridization assembly zone. Hence, it would be highly valuable to develop a novel chemical-modification-based strategy for dynamic DNA self-assembly with the regulating group outside of the hybridization assembly zone, achieving more versatile and facile dynamic controls.

In the present strategy, we design a single-stranded loop (named the control loop) that hangs over the hybridization block, and the states of the loop can regulate the assembly and disassembly of DNA structures. As shown in Scheme 1a, when the loop is intact or formed, DNA tiles can associate with each other through sticky ends (marked in blue and aqua), resulting in the self-assembly of designed nanostructures. Conversely, when the loop is cleaved into two separated overhangs, the tiles cannot associate with each other for higher-order self-assembly, because the existence of overhangs close to the sticky ends would largely weaken the interactions between tiles and hinder the formation of the target DNA nanostructure. The control loop is embedded with responsive chemical groups, which could respond to stimulus and determine whether the loop is formed or cleaved, achieving the dynamic

Anhui Province Key Laboratory of Value-Added Catalytic Conversion and Reaction Engineering, Anhui Province Engineering Research Center of Flexible and Intelligent Materials, School of Chemistry and Chemical Engineering, Hefei University of Technology, Hefei, Anhui 230009, China. E-mail: liyulin@hfut.edu.cn

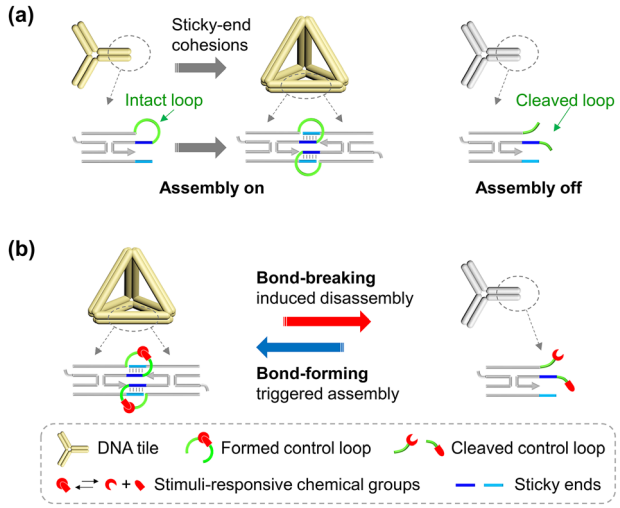

Scheme 1 Schematic diagram of dynamic DNA self-assembly controlled by a loop embedded with responsive chemical groups. (a) The states of the loop determine the self-assembly of DNA tiles. When the loop is intact, DNA self-assembly occurs through sticky-end cohesion. When the loop is cleaved, the assembly process is prevented. (b) Stimuli-responsive chemical groups are embedded in the loop to dynamically control the states of the loop. Stimuli-triggered assembly and disassembly of DNA nanostructures are thus achieved by forming and breaking the responsive covalent bonds in the loop region, respectively.

control of the assembly and disassembly of DNA nanostructures (Scheme 1b).

2. Materials and methods

2.1. Chemicals and reagents

Tris(hydroxymethyl) aminomethane (Tris), ethylenediamine tetraacetic acid disodium salt (EDTA·Na_2), magnesium acetate ($MgAc_2$), sodium acetate (NaAc), L-sodium ascorbate (L-AA), tris-(2-carboxyethyl)-phosphine hydrochloride (TCEP), acrylamide and bis-acrylamide were purchased from Sangon Bioengineering Technology and Services Co. Ltd (Shanghai, China). Acetic acid (HAc), hydrogen peroxide (H_2O_2), copper(II) sulfate ($CuSO_4·5H_2O$) and formamide were obtained from Sinopharm Chemical (Shanghai, China).

2.2. Oligonucleotides

All strands were purchased from Sangon Bioengineering Technology and Services Co. Ltd (Shanghai, China). The strand of Y1 for the assembly of a tetrahedron was cyclized by enzymatic ligation and purified by denaturing polyacrylamide gel electrophoresis. Other strands were used directly without purification.

2.3. Thermal annealing for DNA self-assembly

For the self-assembly of double-crossover (DX) tiles, all constituent DNA strands were mixed in a 1× TAE/Mg buffer (40 mM Tris, 20 mM HAc, 2 mM EDTA·Na_2, 12.5 mM $MgAc_2$, pH 8.0), followed by a fast thermal annealing process (95 °C for 3 minutes, 65 °C for 5 minutes, 50 °C for 10 minutes, 37 °C for 10 minutes, and room temperature (RT) for 10 minutes). For the self-assembly of three-point-star tiles (Y-tiles), all constituent DNA strands were mixed in a 1× TAE/Na buffer (40 mM Tris, 20 mM HAc, 2 mM EDTA·Na_2, and 200 mM NaAc, pH 8.0), followed by a slow thermal annealing process from 95 °C to RT overnight in a 1-litre water bath insulated in a styrofoam box. The concentration of the DX tile or Y-tile was 200 nM.

2.4. UV light induced disassembly

First, the dimers of **DX-PC** tiles and the DNA tetrahedron composed of **Y-PC** tiles were assembled by thermal annealing in a 1× TAE/Mg buffer and a 1× TAE/Na buffer, respectively. Then, the sample was exposed to UV light (~312 nm) for 5 minutes. Finally, all samples were analyzed by native polyacrylamide gel electrophoresis (native PAGE).

2.5. Cu^+-triggered assembly

First, all constituent DNA strands for the **DX-CuAAC** tile and the **Y-CuAAC** tile were mixed in a 1× TA/Mg buffer and a 1× TA/Na buffer (without EDTA), respectively, followed by a fast thermal annealing process. Then, Cu^{2+} (0.5 mM) and L-sodium ascorbate (1.0 mM) were added. The samples were incubated at ~17 °C for three hours for the copper-catalyzed azide–alkyne cycloaddition (CuAAC). Finally, all samples were analyzed by native PAGE.

2.6. Redox-responsive reversible assembly and disassembly

First, the dimers of **DX-SS** tiles and the DNA tetrahedron composed of **Y-SS** tiles were assembled by thermal annealing in the 1× TAE/Mg buffer and the 1× TAE/Na buffer, respectively. Then, redox-responsive disassembly and assembly were realized by adding TCEP and H_2O_2 alternately. After each addition, the solution was allowed to sit quietly on the bench at RT (~25 °C) overnight. Finally, all samples were analyzed by native PAGE.

2.7. Native polyacrylamide gel electrophoresis

The gels containing 3% or 6% polyacrylamide (19:1 acrylamide/bisacrylamide) were run on an electrophoresis unit (DYCZ-24DN, Beijing Liuyi Biotechnology Co. Ltd., China) at RT under a constant voltage of 100 V. The gel buffer and running buffer were 1× TAE/Mg. The gels were stained with Stains-All (Sigma) and photographed with a camera after electrophoresis.

2.8. Denaturing PAGE

The gels containing 15% polyacrylamide (19:1 acrylamide/bisacrylamide) and 8.3 M urea were run on a DYCZ-24DN electrophoresis unit at RT under a constant voltage of 250 V. The gel buffer and running buffer were Tris–Borate–EDTA buffer (TBE), which consisted of 89 mM Tris buffer (pH 8.0), 89 mM boric acid, and 2 mM EDTA. DNA samples containing about 50% (v/v) formamide were heated at 95 °C for 3 minutes before being loaded in the gels. After electrophoresis, the gels were stained with Stains-All (Sigma) and photographed with a camera.

2.9. Atomic force microscopy (AFM) characterization

5 μL of the sample was spotted onto a freshly cleaved mica surface. The drop was blown away in 30 seconds by compressed air, followed by washing the surface 1–2 times with 2 mM $MgAc_2$ solution. Then, the samples were imaged in air with a Bruker Dimension Icon atomic force microscope operated in a ScanAsyst mode using a Bruker SNL-10 AFM tip (65 kHz, 0.35 N m^{-1}). All AFM images were produced by the software NanoScopeAnalysis.

3. Results and discussion

3.1. Impact of the control loop on the dimerization of DX tiles

To test the impact of the control loop over DNA assembly, we first compared the dimerization of double-crossover (DX) tiles with cleaved and formed control loops (Fig. 1a and Fig. S1).[42] One terminal of the DX tile was set to be blunt, preventing the polymerization of DX tiles. The other terminal contains the sticky end (marked in blue and aqua in Fig. 1a) and control loop (marked in green in Fig. 1a). The two tiles, named the **DX-T_4** tile and the **DX-T_2/T_2** tile respectively, have the same sticky end of 5 nucleotides (abbreviated as 5-nt) but different control loops. The **DX-T_4** tile has an intact single-stranded loop of four thymine (T) nucleotides. The length of T nucleotides was experimentally optimized to be four by trying a series of different lengths of poly-T loops (Fig. S2). In contrast, the **DX-T_2/T_2** tile, corresponding to the tile with a cleaved control loop, has two separated overhangs, each of which was composed of 2 thymine nucleotides.

Native PAGE analysis results in Fig. 1b and Fig. S3b showed that the **DX-T_4** tile could self-assemble into the dimeric nanostructure through Watson–Crick base pair interactions. However, the dimerization of the **DX-T_2/T_2** tile was completely hindered. The sharp contrast demonstrated that the dimerization of DX tiles could be regulated through the control loop. That is, the intact control loop allowed the dimerization, while the cleaved loop impeded the assembly. Since the lengths of sticky ends were crucial for DNA self-assembly, we designed three more groups of sticky ends with various lengths, including 7-, 6-, and 4-nucleotides (abbreviated as 7-nt, 6-nt, and 4-nt tiles, respectively). Besides, the length of the overhang was also an important factor in our strategy, so we also tried different lengths of overhangs, including 2-, 1- and 0-thymine nucleotides (abbreviated as T_2, T_1, and T_0, respectively). As shown in Fig. 1c and Fig. S3c, although a small amount of dimer products of the **DX-T_2/T_2** tile with a 6-nt sticky end was seen in the gel, the contrast with that of the **DX-T_4** tile was still obvious. The length of overhangs had an obvious impact on the dimerization of DX tiles when the sticky end was 6-nt. The shorter the overhang, the more the dimer products obtained. When the length of the sticky end increased to be 7-nt (Fig. 1d and Fig. S3d), much more dimer products of the **DX-T_2/T_2** tile were observed, resulting in the diminished difference between the self-assembly of the **DX-T_4** tile and the **DX-T_2/T_2** tile. Conversely, when the length of the sticky end was 4-nt, both the **DX-T_4** tile and the **DX-T_2/T_2** tile could not assemble into stable dimeric structures (Fig. S3a). Therefore, an appropriate inter-association strength between DNA tiles would be significant in our strategy.

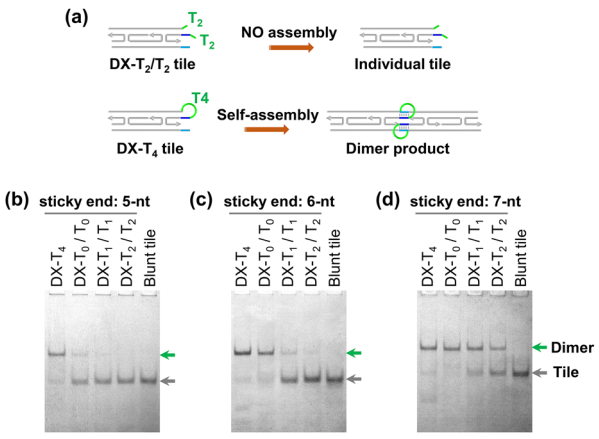

Fig. 1 Dimerization of DX tiles with cleaved and formed control loops. (a) Schematic diagram of the assembly of **DX-T_2/T_2** and **DX-T_4** tiles. 6% native PAGE analysis of the self-assembly products of **DX-T_2/T_2** and **DX-T_4** tiles with the sticky ends of (b) 5-nt, (c) 6-nt, and (d) 7-nt.

3.2. Impact of the control loop on the assembly of a tetrahedron

To further check the feasibility of our strategy, we moved forward to investigate the impact of the control loop on the assembly of a wireframe tetrahedron (*TET*), a higher-order DNA nanostructure composed of four copies of a symmetric three-point-star tile (Y-tile).[43,44] As shown in Fig. 2a and Fig. S4, all

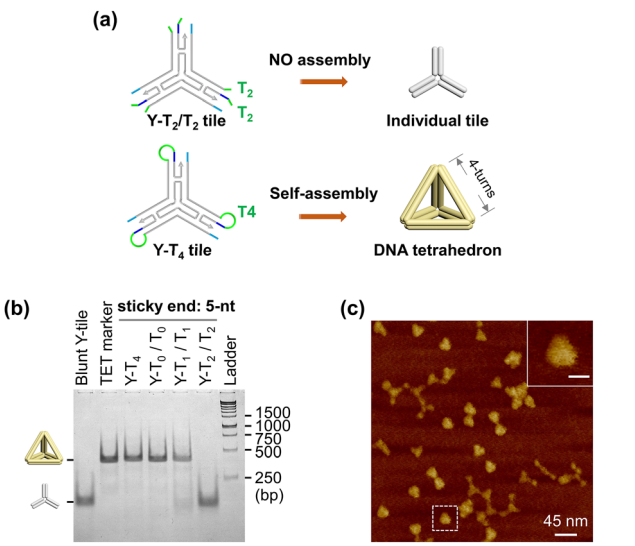

Fig. 2 Assembly of a *TET* from Y-tiles with cleaved and intact control loops. (a) Schematic diagram of the assembly of **Y-T_2/T_2** and **Y-T_4** tiles. The length of each edge of the *TET* was four turns (42 base-pairings). (b) 3% native PAGE analysis of the self-assembly products of **Y-T_2/T_2** and **Y-T_4** tiles with a 5-nt sticky end. (c) Atomic force microscopy (AFM) image of the assembly products of the **Y-T_4** tile. The inset shows a close-up view of the particle marked with a white square. The scale bar in the inset is 15 nm.

three branches of the Y-tile have the sticky end and control loop. Each branch of the **Y-T_4** tile has an intact single-stranded loop of 4T nucleotides, while each branch of the **Y-T_2/T_2** tile has two separated overhangs of 2T nucleotides, representing the tile with a cleaved control loop. The two tiles have the same sticky end of 5-nt. As demonstrated by the native PAGE data (Fig. 2b) and atomic force microscopy (AFM) results (Fig. 2c and Fig. S5), the **Y-T_4** tiles can associate with each other to assemble into the designed DNA tetrahedron. In contrast, no *TET* product was seen in the gel when using the **Y-T_2/T_2** tile (Fig. 2b). The influences of the lengths of sticky ends were also studied (Fig. S6 and S7). When the sticky end was 6-nt, the contrast between the self-assembly of the **Y-T_4** tile and the **Y-T_2/T_2** tile was striking, similar to the results of 5-nt tiles. However, when the inter-association strength was too weak (4-nt sticky end) or too strong (7-nt sticky end), the difference between the self-assembly of the **Y-T_4** tile and the **Y-T_2/T_2** tile diminished.

3.3. Stimuli-responsive dimerization of DX tiles

The above results proved that the self-assembly of DNA nanostructures through the inter-association of DNA tiles could be controlled by the single-stranded control loop in the tile. When the control loop was formed, DNA tiles could associate with each other through the hybridization of sticky ends to form higher-order DNA nanostructures. Conversely, when the loop was cleaved into separated overhangs, the self-assembly of the DNA nanostructure would be significantly hindered. Based on the above findings, we further considered incorporating stimuli-responsive chemical groups into the control loop to realize dynamic regulation of DNA self-assembly. The great variety of responsive chemical groups would make diverse regulation models possible. Stimuli-responsive dimerization of DX tiles was first chosen as an example.

We first tested the "Turn-Off" system, that is, the disassembly of as-formed DNA nanostructures resulting from the cleavage of the control loop when exposed to a stimulus. As shown in Fig. 3a and Fig. S8a, a photocleavable *o*-nitrobenzyl group was inserted into the control loop of the DX tile,[37–39] named the **DX-PC** tile. After UV light irradiation, the native PAGE analysis (Fig. 3b and Fig. S9a) results showed a clear downshifted band which matched the electrophoretic speed of the individual DX tile, indicating the disassembly of dimeric nanostructures. The cleavage of the *o*-nitrobenzyl-labeled loop strand was confirmed by the denaturing PAGE analysis of the products after UV light irradiation (Fig. S10). Conversely, the as-formed dimer without UV light irradiation did not disassociate into the individual DX tile. The control sample of the **DX-T_4** tile, which did not contain the *o*-nitrobenzyl group, still ran at the speed of the dimers in the gel even after UV light irradiation (Fig. 3b and Fig. S9b). The percentages of the dimeric nanostructures were roughly estimated from the band intensity using Image J software (Fig. 3c).[45] It showed a significant decrease in the percentage of the dimeric assembly products of **DX-PC** tiles after UV light irradiation. These results demonstrated that responsive disassembly of the DNA nanostructure can be achieved by inserting a stimuli-induced cleavable group in the control loop of the DNA tile.

We further demonstrated the "Turn-On" system, that is, DNA nanostructures were assembled from the tiles after the formation of the covalently linked control loop from two separated overhangs when exposed to a stimulus. Click chemistry is renowned for its high efficiency and specificity in chemical synthesis.[41,46] Therefore, we designed such a "Turn-On" system using the click reactions of strain-promoted azide–alkyne cycloaddition reaction (SPAAC) and copper-catalyzed azide–alkyne cycloaddition reaction (CuAAC).[47–49] As shown in Fig. S8b, the **DX-AAC** tile was composed of an azide-labelled strand, a dibenzocyclooctyn (DBCO)-labelled strand and three other unlabelled strands. In the **DX-CuAAC** tile, the DBCO-labelled strand was replaced by an alkyne-labelled strand (Fig. 3d and Fig. S8c). After a thermal annealing process, dimeric nanostructures were obtained using the **DX-AAC** tile,

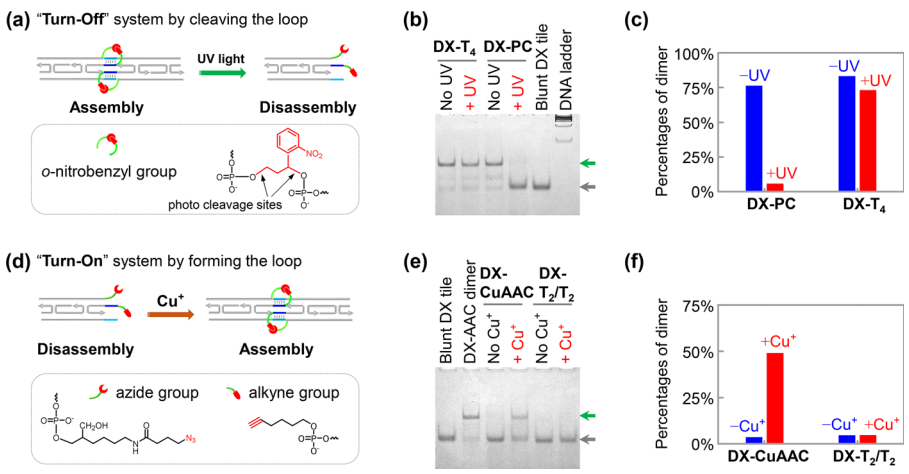

Fig. 3 Stimuli-responsive disassembly and assembly of DX tiles. (a) Schematic diagram and (b) 6% native PAGE analysis of UV-light-induced disassembly of the dimeric nanostructure of the **DX-PC** tile. (c) Quantitative analysis of the gel result in (b). (d) Schematic diagram and (e) 6% native PAGE analysis of Cu^+-triggered dimerization of the **DX-CuAAC** tile. (f) Quantitative analysis of the gel result in (e).

because the control loop could be formed through DBCO-azide conjugation without the need for a catalyst. However, individual tiles rather than the dimeric nanostructures were obtained when using the **DX-CuAAC** tile, since the azide- and alkyne-groups were unable to be covalently linked to form the intact control loop in the absence of a Cu^{+} catalyst. Upon the addition of a Cu^{+} catalyst, which was *in situ* generated through the reduction of Cu^{2+} by sodium ascorbate, the click chemistry between azide- and alkyne-groups was initiated, resulting in the formation of the intact control loop. Thanks to the proximity effect, the reaction between azide- and alkyne-groups within one tile has great precedence over the linkage of azide- and alkyne-groups between two tiles (Fig. S11), forming the loop as desired and therefore triggering the dimerization of **DX-CuAAC** tiles. As shown by the native PAGE results in Fig. 3e and Fig. S12, an upshifted band that matched the electrophoretic speed of the dimer marker appeared after adding Cu^{+}, indicating the dimerization of **DX-CuAAC** tiles through the formation of the control loop by the CuAAC reaction. The linkage of the azide-labelled strand and the alkyne-labelled strand was confirmed by the denaturing PAGE analysis of the products after Cu^{+} treatment (Fig. S13). The reaction could be finished in several minutes (Fig. S14). When adding the Cu^{+} catalyst to the control sample of **DX-T_2/T_2** tiles without azide- and alkyne-groups, no dimeric products were seen in the gel (Fig. 3e). The quantitative analysis of the gel image in Fig. 3e showed a substantial increase in the percentage of the dimeric nanostructures after adding the Cu^{+} catalyst to the sample of **DX-CuAAC** tiles (Fig. 3f).[45] These results proved that click reactions can be applied for the covalent linkage of two adjacent overhangs to form the intact control loop in the tile, thus triggering the self-assembly of DNA tiles into higher-order nanostructures. Any stimulus initiating the click reactions could, in principle, be developed for such "Turn-On" control of DNA self-assembly.

To move one step forward, we further designed an "On–Off–On" system, that is, to achieve the reversible self-assembly and disassembly cycles of the DNA nanostructure when exposed to specific stimuli through regulating the formation and cleaving of the control loop reversibly. Dynamic covalent chemistry relates to

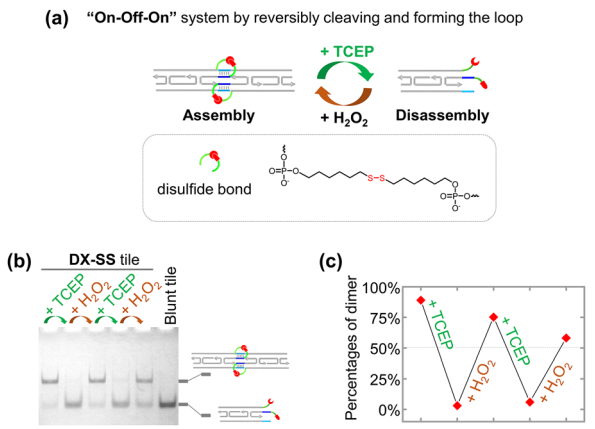

Fig. 4 Redox-responsive reversible self-assembly of a **DX-SS** tile. (a) Schematic diagram. (b) 6% native PAGE analysis of three cycles of the assembly and disassembly of **DX-SS** tiles. (c) Quantitative analysis of the gel result in (b).

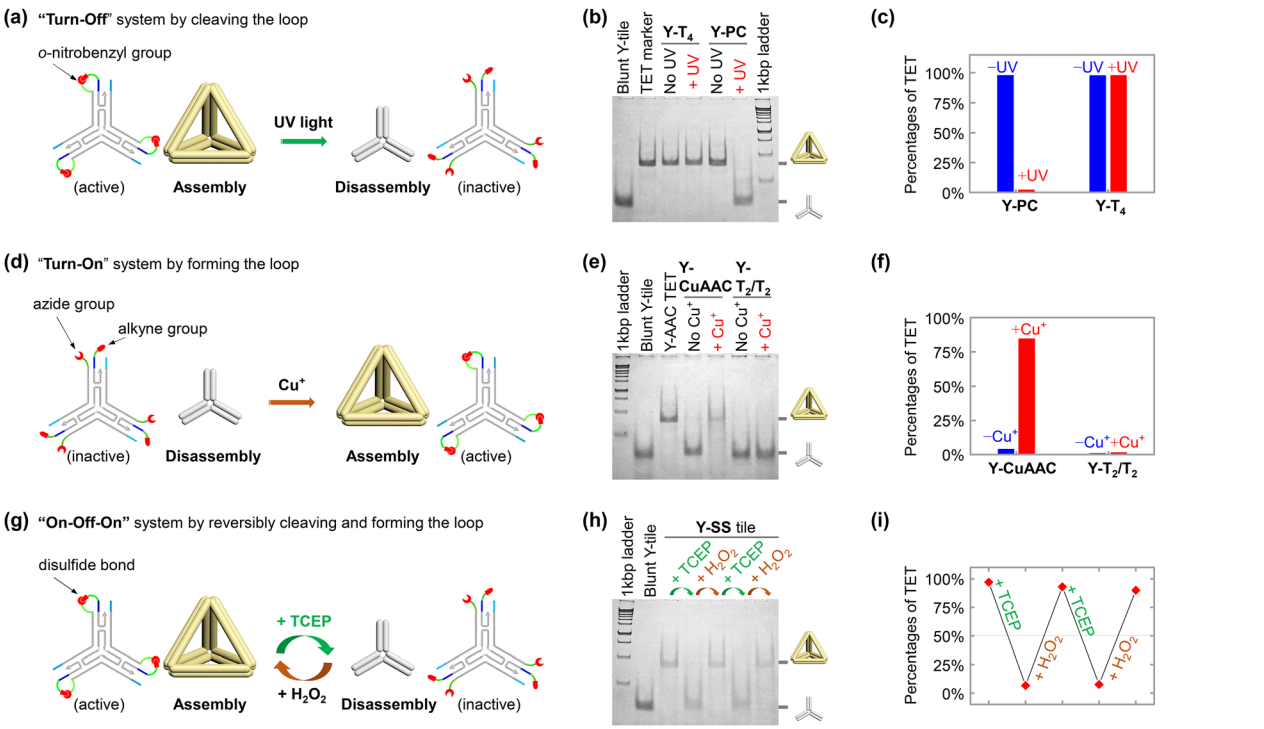

Fig. 5 Stimuli-responsive self-assembly of (a)–(c) the **Y-PC** tile, (d)–(f) the **Y-CuAAC** tile and (g)–(i) the **Y-SS** tile. (a), (d) and (g) Schematic diagrams. (b), (e) and (h) 3% native PAGE analysis. (c), (f) and (i) Quantitative analysis results of the gel images in (b), (e) and (h), respectively.

the chemical reactions that could be carried out reversibly under appropriate conditions.[50] Therefore, we tried to insert a dynamic covalent bond into the control loop to realize the "On–Off–On" regulation. We chose the disulfide bond as an example, since it has been extensively studied and widely applied in dynamic covalent chemistry and also plays an extremely significant role in biological systems.[51,52] A disulfide bond was inserted into the control loop of the DX tile, and the as-obtained tile was named the **DX-SS** tile (Fig. 4a and Fig. S8d). As shown in Fig. 4b and Fig. S15, **DX-SS** tiles assembled into the dimeric nanostructures because the control loop was intact. Upon the addition of the reductant (*e.g.*, TCEP), the band corresponding to dimers disappeared and a new downshifted band matching the electrophoretic speed of DX tiles appeared, indicating the disassembly of the dimeric nanostructures. The reason was that the breaking of the disulfide bond cleaved the control loop into two separated overhangs. Subsequently, after adding the oxidant (*e.g.*, H_2O_2) to trigger the formation of the disulfide bond, the dimers of **DX-SS** tiles were re-assembled due to the formation of the control loop. Three cycles of disassembly and re-assembly of the dimeric nanostructures of **DX-SS** tiles have been demonstrated (Fig. 4b). The quantitative analysis results of the cycles are shown in Fig. 4c.[45] The cleavage and linkage of the disulfide-bond-containing control loop were confirmed by the denaturing PAGE analysis of the products in the first cycle (Fig. S16). Moreover, the speed of reversible assembly and disassembly of the dimeric nanostructures of **DX-SS** tiles could be regulated by varying the concentrations of the additives (Fig. S17 and S18). Hence, we have demonstrated the feasibility of designing reversible "On–Off–On" DNA self-assembly systems through integrating dynamic covalent bonds in the control loop.

3.4. Stimuli-responsive self-assembly of a DNA *TET*

After establishing the "Turn-Off", "Turn-On", and "On–Off–On" dynamic regulation systems for the dimerization of DX-tiles, we further realized the corresponding dynamic systems for the assembly of a three-dimensional tetrahedron through inserting the stimuli-responsive chemical groups into the control loop (Fig. 5 and Fig. S19). By incorporating the photocleavable *o*-nitrobenzyl group into the control loop, the disassembly of the DNA *TET* was specifically triggered by UV light irradiation (Fig. 5a–c and Fig. S20). The Cu^+-triggered self-assembly of DNA *TET* was achieved by using the three-point-star tile labelled with azide- and alkyne-groups (Fig. 5d–f and Fig. S21, S22). Cycles of reversible assembly and disassembly of the DNA *TET*, through forming and breaking the disulfide bond embedded in the control loop upon the addition of an oxidant (*e.g.*, H_2O_2) and a reductant (*e.g.*, TCEP) alternatively, have also been demonstrated (Fig. 5g–i and Fig. S23).

4. Conclusions

In conclusion, we have demonstrated a facile and versatile strategy for dynamic DNA self-assembly through a control loop embedded with responsive chemical groups. When the loop is formed/intact, the DNA assembly can occur; however, when the loop is cleaved, the DNA assembly is significantly impeded. The "Turn-On", "Turn-Off", and reversible "On–Off–On" systems have been rationally designed for both the dimerization of DX tiles and the assembly of a DNA tetrahedron. Various stimuli, including light irradiation, metal ions (*e.g.*, Cu^+), and small molecules (*e.g.*, TCEP and H_2O_2), have been employed in our design. The advantages of our strategy are as follows. First, the control loop in our strategy is not part of the hybridization zone of the assembly, which means the control loop is not directly involved in hybridization. The relative independence between the control unit and the assembly unit endows the current strategy with more designability and versatility. Second, thanks to the great variety of responsive chemical groups and dynamic covalent chemistry,[38,41,46,50] our strategy could in principle be widely expanded to achieve diverse regulation models. In addition, the rational design of incorporating multiple chemical groups into one system or coupling with other regulation tools makes complex controls on DNA self-assembly possible, holding great potential in a wide range of applications, such as dissipative self-assembly,[36] molecular robots,[11,12,14] DNA computing,[20,21,23,24] and *in vivo* targeted imaging and drug-delivery,[2,3,5,9] which demand smart DNA assemblies that can respond to one or multiple specific stimuli as required. Our strategy will greatly enrich the current regulation pool and bring new benefits for dynamic DNA nanotechnology.

Author contributions

Zhiyuan Zhu: investigation and methodology; Mengzhou Wei: investigation; and Yulin Li: conceptualization, supervision, writing – original draft and writing – review & editing.

Conflicts of interest

There are no conflicts to declare.

Data availability

Supplementary data associated with this article are available in the supplementary information (SI). Supplementary information is available. See DOI: **https://doi.org/10.1039/d5nh00609k**.

Acknowledgements

This work was supported by the National Natural Science Foundation of China (grant No. 21971053). We thank Prof. Cuiming Wu from Hefei University of Technology for the kind help on AFM characterization.

References

1 N. C. Seeman and H. F. Sleiman, *Nat. Rev. Mater.*, 2017, **3**, 17068.
2 Q. Hu, H. Li, L. Wang, H. Gu and C. Fan, *Chem. Rev.*, 2019, **119**, 6459–6506.
3 S. Yu, Y. Xie, Y. Jiao, N. Li and B. Ding, *Nanoscale Horiz.*, 2025, **10**, 1802–1814.

4 J. Wang, Z. Li and I. Willner, *Angew. Chem., Int. Ed.*, 2023, **62**, e202215332.
5 N. Song, H. Li, C. Yao and D. Yang, *Acc. Chem. Res.*, 2024, **57**, 2763–2774.
6 S. He, J. Shang, Y. He and F. Wang, *Acc. Chem. Res.*, 2024, **57**, 533–544.
7 F. He, M. Wang, J. Wang, H. Wang and Z. Nie, *Angew. Chem., Int. Ed.*, 2023, **62**, e202305227.
8 M. Zhang, C. Yancey, C. Zhang, J. Wang, Q. Ma, L. Yang, R. Schulman, D. Han and W. Tan, *Sci. Adv.*, 2024, **10**, eadn3329.
9 H. Zhao, D. Yi, L. Li, Y. Zhao and M. Li, *Angew. Chem., Int. Ed.*, 2024, **63**, e202404064.
10 S. Fan, S. Wang, L. Ding, T. Speck, H. Yan, S. Nussberger and N. Liu, *Nat. Mater.*, 2025, **24**, 278–286.
11 H. Ramezani and H. Dietz, *Nat. Rev. Genet.*, 2020, **21**, 5–26.
12 S. Cao, F. Wang, L. Wang, C. Fan and J. Li, *Nanoscale Horiz.*, 2022, **7**, 578–588.
13 L. N. Green, H. K. K. Subramanian, V. Mardanlou, J. Kim, R. F. Hariadi and E. Franco, *Nat. Chem.*, 2019, **11**, 510–520.
14 A. J. Thubagere, W. Li, R. F. Johnson, Z. Chen, S. Doroudi, Y. L. Lee, G. Izatt, S. Wittman, N. Srinivas, D. Woods, E. Winfree and L. Qian, *Science*, 2017, **357**, eaan6558.
15 S. F. J. Wickham, J. Bath, Y. Katsuda, M. Endo, K. Hidaka, H. Sugiyama and A. J. Turberfield, *Nat. Nanotechnol.*, 2012, **7**, 169–173.
16 C. Zhang, X. Ma, X. Zheng, Y. Ke, K. Chen, D. Liu, Z. Lu, J. Yang and H. Yan, *Sci. Adv.*, 2022, **8**, eabl4589.
17 M. Kim, C. Lee, K. Jeon, J. Y. Lee, Y. Kim, J. G. Lee, H. Kim, M. Cho and D. Kim, *Nature*, 2023, **619**, 78–86.
18 Y. Ke, T. Meyer, W. M. Shih and G. Bellot, *Nat. Commun.*, 2016, **7**, 10935.
19 L. Zhou, Y. Xiong, A. Dwivedy, M. Zheng, L. Cooper, S. Shepherd, T. Song, W. Hong, L. T. P. Le, X. Chen, S. Umrao, L. Rong, T. Wang, B. T. Cunningham and X. Wang, *Sci. Robot.*, 2024, **9**, eadi2084.
20 J. Seo, S. Kim, H. H. Park and J. Nam, *Small*, 2019, **15**, 1900998.
21 J. Shu, Z. H. Tan, Q. Wang and K. Yong, *J. Am. Chem. Soc.*, 2023, **145**, 25033–25042.
22 H. Kang, T. Lin, X. Xu, Q. Jia, R. Lakerveld and B. Wei, *Nat. Commun.*, 2021, **12**, 4994.
23 X. Liu, D. Yao, Y. Wang, D. Ni, W. Hua, J. Tian, L. Yang, H. Lin, H. Liang and Z. Deng, *J. Am. Chem. Soc.*, 2024, **146**, 30573–30583.
24 Y. Pei, T. Bian, Y. Liu, Y. Liu, Y. Xie and J. Song, *Nano Lett.*, 2022, **22**, 3003–3010.
25 Y. Yu, B. Jin, Y. Li and Z. Deng, *Chem. – Eur. J.*, 2019, **25**, 9785–9798.
26 F. C. Simmel, B. Yurke and H. R. Singh, *Chem. Rev.*, 2019, **119**, 6326–6369.
27 X. Yan, Y. Wang, N. Ma, Y. Yu, L. Dai and Y. Tian, *J. Am. Chem. Soc.*, 2023, **145**, 3978–3986.
28 X. Zhang, R. Du, S. Xu, X. Wang and Z. Wang, *Nanoscale Horiz.*, 2024, **9**, 1582–1586.
29 J. W. Conway, C. Madwar, T. G. Edwardson, C. K. Mclaughlin, J. Fahkoury, R. B. Lennox and H. F. Sleiman, *J. Am. Chem. Soc.*, 2014, **136**, 12987–12997.
30 X. Chang, Q. Yang, J. Y. Lee, D. Perumal and F. Zhang, *J. Am. Chem. Soc.*, 2024, **146**, 26131–26138.
31 Y. Dong, Z. Yang and D. Liu, *Acc. Chem. Res.*, 2014, **47**, 1853–1860.
32 A. Amodio, A. F. Adedeji, M. Castronovo, E. Franco and F. Ricci, *J. Am. Chem. Soc.*, 2016, **138**, 12735–12738.
33 Q. Li, L. Liu, D. Mao, Y. Yu, W. Li, X. Zhao and C. Mao, *J. Am. Chem. Soc.*, 2020, **142**, 665–668.
34 J. Dong, M. P. O'Hagan and I. Willner, *Chem. Soc. Rev.*, 2022, **51**, 7631–7661.
35 Y. Suzuki, M. Endo, Y. Yang and H. Sugiyama, *J. Am. Chem. Soc.*, 2014, **136**, 1714–1717.
36 E. D. Grosso, L. J. Prins and F. Ricci, *Angew. Chem., Int. Ed.*, 2020, **59**, 13238–13245.
37 D. Perumal, Q. Yang, M. Jeziorek, J. Y. Lee, J. Etchegaray and F. Zhang, *ACS Appl. Opt. Mater.*, 2025, **3**, 507–513.
38 M. P. O'Hagan, Z. Duan, F. Huang, S. Laps, J. Dong, F. Xia and I. Willner, *Chem. Rev.*, 2023, **123**, 6839–6887.
39 H. Faheem, J. Mathivanan, H. Talbot, H. Zeghal, S. Vangaveti, J. Sheng, A. A. Chen and A. R. Chandrasekaran, *Nucleic Acid Res.*, 2023, **51**, 4055–4063.
40 Z. Zhou, H. Y. Chan and P. K. Lo, *JACS Au*, 2025, **5**, 2953–2976.
41 N. Z. Fantoni, A. H. El-Sagheer and T. Brown, *Chem. Rev.*, 2021, **121**, 7122–7154.
42 T. Fu and N. C. Seeman, *Biochemistry*, 1993, **32**, 3211–3220.
43 Y. He, T. Ye, M. Su, C. Zhang, A. E. Ribbe, W. Jiang and C. Mao, *Nature*, 2008, **452**, 198–201.
44 K. Zhou, Z. Mei, Y. Lei, Z. Guan, C. Mao and Y. Li, *ChemBioChem*, 2022, **23**, e202200138.
45 C. A. Schneider, W. S. Rasband and K. W. Eliceiri, *Nat. Methods*, 2012, **9**, 671–675.
46 J. Li and P. R. Chen, *Nat. Chem. Biol.*, 2016, **12**, 129–137.
47 M. Meldal and C. W. Tornøe, *Chem. Rev.*, 2008, **108**, 2952–3015.
48 V. Cassinelli, B. Oberleitner, J. Sobotta, P. Nickels, G. Grossi, S. Kempter, T. Frischmuth, T. Liedl and A. Manetto, *Angew. Chem., Int. Ed.*, 2015, **54**, 7795–7798.
49 Z. Lin, Y. Xiong, S. Xiang and O. Gang, *J. Am. Chem. Soc.*, 2019, **141**, 6797–6801.
50 Z. Lei, H. Chen, S. Huang, L. J. Wayment, Q. Xu and W. Zhang, *Chem. Rev.*, 2024, **124**, 7829–7906.
51 M. H. Lee, Z. Yang, C. W. Lim, Y. H. Lee, S. Dongbang, C. Kang and J. S. Kim, *Chem. Rev.*, 2013, **113**, 5071–5109.
52 D. J. Hansen, J. Manuguerra, M. B. Kjelstrup and K. V. Gothelf, *Angew. Chem., Int. Ed.*, 2014, **53**, 14415–14418.

